This is an electronic reprint of the original article.
This reprint *may differ* from the original in pagination and typographic detail.

Author(s): Klesko, Joseph P.; Bellow, James A.; Saly, Mark J.; Winter, Charles H.; Julin, Jaakko; Sajavaara, Timo

Title: Unusual stoichiometry control in the atomic layer deposition of manganese borate films from manganese bis(tris(pyrazolyl)borate) and ozone

Year: 2016

Version:

Please cite the original version:

Klesko, J. P., Bellow, J. A., Saly, M. J., Winter, C. H., Julin, J., & Sajavaara, T. (2016). Unusual stoichiometry control in the atomic layer deposition of manganese borate films from manganese bis(tris(pyrazolyl)borate) and ozone. Journal of Vacuum Science and Technology A, 34(5), Article 051515. https://doi.org/10.1116/1.4961385

All material supplied via JYX is protected by copyright and other intellectual property rights, and duplication or sale of all or part of any of the repository collections is not permitted, except that material may be duplicated by you for your research use or educational purposes in electronic or print form. You must obtain permission for any other use. Electronic or print copies may not be offered, whether for sale or otherwise to anyone who is not an authorised user.

Unusual stoichiometry control in the atomic layer deposition of manganese borate films from manganese bis(tris(pyrazolyl)borate) and ozone

Joseph P. Klesko, James A. Bellow, Mark J. Saly, Charles H. Winter, Jaakko Julin, and Timo Sajavaara

Citation: Journal of Vacuum Science & Technology A **34**, 051515 (2016); doi: 10.1116/1.4961385
View online: http://dx.doi.org/10.1116/1.4961385
View Table of Contents: http://scitation.aip.org/content/avs/journal/jvsta/34/5?ver=pdfcov
Published by the AVS: Science & Technology of Materials, Interfaces, and Processing

Articles you may be interested in
Low-temperature atomic layer deposition of copper(II) oxide thin films
J. Vac. Sci. Technol. A **34**, 01A109 (2016); 10.1116/1.4933089

Nucleation and growth of ZnO on PMMA by low-temperature atomic layer deposition
J. Vac. Sci. Technol. A **33**, 01A128 (2015); 10.1116/1.4902326

Low temperature silicon dioxide by thermal atomic layer deposition: Investigation of material properties
J. Appl. Phys. **107**, 064314 (2010); 10.1063/1.3327430

The impact of the density and type of reactive sites on the characteristics of the atomic layer deposited W N x C y films
J. Appl. Phys. **99**, 063515 (2006); 10.1063/1.2182074

Atomic layer deposition of nickel oxide films using Ni (dmamp) 2 and water
J. Vac. Sci. Technol. A **23**, 1238 (2005); 10.1116/1.1875172

Redistribution subject to AVS license or copyright; see http://scitation.aip.org/termsconditions. IP: 130.234.75.50 On: Mon, 12 Sep 2016 08:58:03

Unusual stoichiometry control in the atomic layer deposition of manganese borate films from manganese bis(tris(pyrazolyl)borate) and ozone

Joseph P. Klesko,[a] James A. Bellow, Mark J. Saly,[b] and Charles H. Winter[c]
Department of Chemistry, Wayne State University, Detroit, Michigan 48202

Jaakko Julin and Timo Sajavaara
Department of Physics, University of Jyväskylä, 40014 Jyväskylä, Finland

(Received 18 May 2016; accepted 1 August 2016; published 25 August 2016)

The atomic layer deposition (ALD) of films with the approximate compositions $Mn_3(BO_3)_2$ and CoB_2O_4 is described using $MnTp_2$ or $CoTp_2$ [Tp = tris(pyrazolyl)borate] with ozone. The solid state decomposition temperatures of $MnTp_2$ and $CoTp_2$ are ∼370 and ∼340 °C, respectively. Preparative-scale sublimations of $MnTp_2$ and $CoTp_2$ at 210 °C/0.05 Torr afforded >99% recoveries with <0.1% nonvolatile residues. Self-limited ALD growth was demonstrated at 325 °C for $MnTp_2$ or $CoTp_2$ with ozone as the coreactant. The growth rate for the manganese borate process was 0.19 Å/cycle within the ALD window of 300–350 °C. The growth rate for the cobalt borate process was 0.39–0.42 Å/cycle at 325 °C. X-ray diffraction of the as-deposited films indicated that they were amorphous. Atomic force microscopy of 35–36 nm thick manganese borate films grown within the 300–350 °C ALD window showed root mean square surface roughnesses of 0.4–0.6 nm. Film stoichiometries were assessed by x-ray photoelectron spectroscopy and time of flight-elastic recoil detection analysis. The differing film stoichiometries obtained from the very similar precursors $MnTp_2$ and $CoTp_2$ are proposed to arise from the oxidizing ability of the intermediate high valent manganese oxide layers and lack thereof for cobalt. © *2016 American Vacuum Society*.
[http://dx.doi.org/10.1116/1.4961385]

I. INTRODUCTION

Main group metal borates are important nonlinear optical materials.[1–4] Recently, first row transition metal borates have emerged as dioxygen (O_2) evolution catalysts,[5–16] cathode materials in lithium ion batteries,[17–22] catalysts for H_2 production by hydrolysis of sodium borohydride,[23] and superhydrophilic $Ni_3(BO_3)_2$ layers.[24] For many applications, metal borates must be grown as thin films. Cobalt borate and nickel borate films were electrodeposited from solutions of the metal ions in the presence of borate buffers,[5–16] while nanowhiskers of $Ni_3(BO_3)_2$ were grown on nickel substrates by a molten salt method.[24] Metal borate film growth by gas phase processes is complicated by the high vapor pressure of B_2O_3, which makes it generally difficult to control the metal to boron ratios in the thin films at the high temperatures required for growth. For example, BaB_2O_4 films were grown by chemical vapor deposition (CVD) using direct liquid injection of $Ba(thd)_2$(tetraglyme) (thd = 2,2,6,6–tetramethylheptanedionate) and $B(OiPr)_3$ solutions, with O_2 and nitrous oxide as the oxidizer gases.[25] Film growth was achieved between 640 and 840 °C, but a 1:2.5 barium to boron precursor stoichiometry was required to obtain BaB_2O_4 films. Thin films of $Mg_2B_2O_5$ (Ref. 26) and BaB_2O_4 (Ref. 27) were grown by CVD using $MgTp_2$ and $[BaTp_2]_2$ (Ref. 28) [Tp = tris(pyrazolyl)borate], respectively, at temperatures between 750 and 900 °C with O_2 as the coreactant. The Tp ligands provided the boron atoms, but the 2:1 boron to metal stoichiometry in $MgTp_2$ was not retained in the $Mg_2B_2O_5$ films.[26] We previously reported the atomic layer deposition (ALD) of MB_2O_4 films (M = Ca, Sr, Ba) between 250 and 400 °C using $CaTp_2$, $SrTp_2$, and $Ba(TpEt_2)_2$ as the metal and boron precursors with water as the oxygen source.[29–31] Significantly, the 2:1 boron to metal ratio in the precursors was retained in the MB_2O_4 films. ALD uniquely enables the stoichiometry control, since the depositions are conducted below the thermal decomposition temperatures of $CaTp_2$, $SrTp_2$, and $Ba(TpEt_2)_2$ [<400 °C (Ref. 28)]. The intermediate physisorbed precursor monolayers replicate the 2:1 boron to metal precursor stoichiometry in the thin films upon treatment with the water coreactant, and the MB_2O_4 layers are stable to B_2O_3 loss at <400 °C.[29–31] ALD affords conformal coverage of nanoscale features and enables subnanometer control of film thicknesses because of the self-limited growth mechanism.[32,33] ALD can also provide conformal coatings on many nanoscale materials.[34] ALD growth from various bimetallic precursors does not generally replicate the precursor element stoichiometries in the resultant thin films.[35–38]

Given the increasing importance of first row transition metal borates,[5–24] we sought to extend our studies of group 2 MB_2O_4 films by exploring transition metal MTp_2 precursors. Herein, we report the ALD growth of films with the approximate compositions $Mn_3(BO_3)_2$ and CoB_2O_4 using $MnTp_2$ (**1**) and $CoTp_2$ (**2**) as precursors with ozone as the oxygen source. In analogy with the group 2 borate films, use of **2** and ozone affords the expected CoB_2O_4 stoichiometry. In contrast, **1** and ozone give films of the approximate stoichiometry $Mn_3(BO_3)_2$. This differing borate stoichiometry is

[a]Present address: Department of Materials Science and Engineering, University of Texas at Dallas, Richardson, Texas 75080-3021.
[b]Present address: Applied Materials, Santa Clara, California 95054-3318.
[c]Electronic mail: chw@chem.wayne.edu

Redistribution subject to AVS license or copyright; see http://scitation.aip.org/termsconditions. IP: 130.234.75.50 On: Mon, 12 Sep 2016 08:58:03

proposed to arise from the strong oxidizing properties of higher valent manganese oxide layers that are formed upon ozonolysis of surface manganese sites.

II. EXPERIMENT

See supplementary material for details relating to the precursor properties of **1** and **2**, ALD growth data, and film characterization.[39]

Synthetic manipulations were carried out under argon using either Schlenk or glove box techniques in the handling of potassium borohydride for the synthesis of KTp. KTp, **1**, and **2** were synthesized according to literature procedures.[40] Tetrahydrofuran was distilled from sodium benzophenone ketyl and sodium metal. Toluene was distilled from sodium metal. All chemicals were obtained from Sigma Aldrich. The melting points and thermal decomposition temperatures of **1** and **2** were assessed using a Thermo Scientific Mel-Temp 3.0 digital melting point apparatus and are uncorrected. Thermogravimetric (TGA) and differential thermal (DTA) analyses were conducted on a Perkin-Elmer Pyris 1 TGA system between 50 and 450 °C using dinitrogen (N_2) as the flow gas with a heating rate of 10 °C/min. For data, see the supplementary material.

The preparative sublimations of **1** and **2** employed a 2.5 cm diameter, 30 cm long glass tube. One end of the tube was sealed, and the other end was equipped with a vacuum adapter with a 24/40 male glass joint. Approximately 1.0 g of the sample was loaded into a 1.0×4.0 cm glass tube and this tube was placed at the sealed end of the glass sublimation tube. The sublimation tube was fitted with a 24/40 vacuum adapter and was inserted into a horizontal Büchi B-580 or B-585 Kugelrohr oven, such that about 15 cm of the tube was situated in the oven. A vacuum of 0.05 Torr was established, and the oven temperature was set to 210 °C. The compounds sublimed to the cool zone just outside of the oven. The percent recovery was obtained by weighing the sublimed product. The percent nonvolatile residue was calculated by weighing the 1.0×4.0 cm glass tube upon completion of the sublimation experiment. For data, see the supplementary material.

A Picosun Oy R-75BE ALD reactor was used for thin film deposition experiments. A Texol GeniSys N_2 generator supplied 99.9995% N_2 as both the carrier and purge gas, with the reactor maintaining a pressure of 6–10 h Pa while under a constant N_2 flow. Ozone was delivered at 500 sccm by an IN USA AC-Series ozone generator operating at 50% power. Precursors **1** and **2** were delivered by a solid state booster with a source temperature of 194 ± 2.0 °C, at the pressure of the reactor. Films were grown on p-type Si(100) wafers with native oxide. Precursor pulse lengths were varied to determine the degree of surface saturation. The substrate temperature was subsequently varied using saturative doses of the precursors.

Film thicknesses were measured by cross-sectional scanning electron microscopy (SEM) using a JEOL-6510LV electron microscope. Growth rates were calculated by dividing the measured film thicknesses by the number of deposition cycles. Film thicknesses were measured at a minimum of three positions on each film to evaluate the uniformity. Atomic force micrographs (AFM) were obtained with a MultiMode Nanoscope IIIa (Digital Instruments, VEECO). The samples were measured using the tapping mode in air with an E scanner with a maximum scanning size of 12 μm at a frequency of 1 or 2 Hz. A Tap150AI-G tip was used, with a resonance frequency of 150 kHz and a force constant of 5 $N m^{-1}$. Surface roughnesses were calculated as root-mean-square (rms) values. X-ray photoelectron (XPS) analyses were performed with a Perkin-Elmer ESCA 5500 system using monochromatized (SiO_2 crystal) Al Kα radiation (15 kV at 15 mA) and a 90° Omni-Focus lens. The typical background pressure during analysis was 1×10^{-9} Torr. An argon ion sputter was used for depth profiling using 3.0 keV, 25 mA emission current, and 10×10^{-3} Pa. The spectrometer was calibrated to the Au4$f_{7/2}$ peak at 83.80 eV, the Cu3$p_{3/2}$ peak at 74.9 eV, and the Cu2$p_{3/2}$ peak at 932.40 eV. A low-energy electron flood gun was used to neutralize the charge by aligning the adventitious carbon (C1s) peak to 284.6 eV. For all samples, a survey spectrum was recorded over a binding energy range of 0 to 1200 eV using a pass energy of 117.4 eV with a scan step of 1.0 eV. High resolution multiplex spectra were obtained using a pass energy of 23.5 eV with a scan step of 0.025 eV. Observed XPS ionizations were compared with reference values.[41] Time of flight-elastic recoil detection (TOF-ERDA) analyses were performed at the University of Jyväskylä, Finland. Manganese-containing films were analyzed using a 6.8 MeV ^{35}Cl beam in mirror geometry (20.5 + 20.5) with a 41° recoil angle time of flight ERD. The cobalt-containing film was measured with an 8.5 MeV ^{35}Cl beam. UV-Vis analyses were performed on a JASCO V-570 UV/VIS/NIR spectrophotometer (Rev. 1.00); reported data are an average of three measurements. Powder x-ray diffraction experiments were performed on a Rigaku R200B 12 kW rotating anode diffractometer, using copper Kα radiation (1.54056 Å) at 40 kV and 150 mA. Reflections were compared with known crystalline phases from the powder diffraction files of the International Center of Diffraction Data using the JADE 5.0 software package. Sheet resistivity measurements were obtained using a Jandel 4-point probe in combination with a Keithley 2400 SourceMeter and a Keithley 2182A Nanovoltmeter. All films passed the Scotch tape test.

III. RESULTS AND DISCUSSION

A. Precursor properties of 1 and 2

The precursors **1** and **2** (Fig. 1) were prepared according to literature procedures.[40] The crystal structures of **1** (Ref. 42) and **2** (Ref. 43) were reported previously, and both exist as octahedral monomers with metal-nitrogen bonds to the 2-nitrogen atoms of the Tp ligands. The suitability of **1** and **2** as ALD precursors was established by melting point and solid state decomposition temperature measurements, preparative sublimations, and TGA and DTA. The solid state decomposition temperatures of **1** and **2** are ~370 and ~340 °C, respectively. Preparative-scale sublimations were

Redistribution subject to AVS license or copyright; see http://scitation.aip.org/termsconditions. IP: 130.234.75.50 On: Mon, 12 Sep 2016 08:58:03

conducted at 210 °C/0.05 Torr on ~1 g samples of **1** and **2** and afforded >99% recoveries with <0.1% nonvolatile residues. Thus, **1** and **2** have useful ALD precursor properties.

B. Manganese borate film growth and analysis

Initial film deposition trials were conducted with **1** and water at 325 °C. In contrast to $CaTp_2$, $SrTp_2$, and $Ba(TpEt_2)_2$,[29–31] negligible film growth was obtained from **1** with water as the coreactant. Accordingly, ozone was used as a more reactive oxygen source. Precursor pulse lengths, substrate temperatures, and the number of cycles were varied to assess the growth behavior. The growth rate was first studied as a function of pulse length of **1** at 325 °C, using 2000 cycles and 5.0 s pulses of ozone with 5.0 s N_2 purges. A plot of growth rate versus pulse length of **1** showed a growth plateau at >5.0 s, affording a saturative growth rate of 0.18 Å/cycle on Si(100) substrates with a native oxide layer [Fig. 2(a)]. A similar plot of growth rate versus ozone pulse length showed saturation at ≥4.0 s with the same growth rate. A pulse sequence of **1** (5.0 s)/N_2 purge (5.0 s)/ozone (5.0 s)/N_2 purge (5.0 s) was thus applied for subsequent depositions. Figure 2(b) shows a plot of growth rate versus temperature for films grown with 2000 cycles, indicating an ALD window between 300 and 350 °C. Increased growth rates for films grown at ≥375 °C appear to arise from thermal decomposition of **1**. A plot of thickness versus number of cycles was linear, with a growth rate of 0.194 Å/cycle. The y-intercept was −3.827 nm, which is close to zero, suggesting efficient nucleation.

The surface morphologies of 35–36 nm thick films grown within the ALD window were quantified by AFM. Films grown at 300 and 325 °C had rms surface roughnesses of 0.4–0.5 nm, while the film grown at 350 °C showed an rms surface roughness of 0.5–0.6 nm (Fig. 3). Accordingly, the film surfaces are very smooth. Cross-sectional SEM revealed smooth, uniform films at all temperatures. A 36 nm thick film deposited at 325 °C showed no reflections in the powder x-ray diffraction spectrum, indicating amorphous material. Films grown at 325 °C were annealed under either N_2 or O_2 atmospheres at 100 °C increments from 400 to 1100 °C for 1 h at each temperature. No crystalline phases were detected for any of these annealed films. Films grown within the ALD window were nonconductive and passed the Scotch tape test.

Compositional analyses were performed on 35–36 nm thick films grown at 300, 325, and 350 °C. XPS survey scans revealed surface carbon and nitrogen contamination in the as-deposited films, which were below the detection limits (<0.5%) after 1 min of argon ion sputtering. The high-resolution spectra of the boron 1s and manganese 2p ionization regions were identical for all films after 2 min of sputtering. Atomic compositions upon sputtering for 2 min were $Mn_{1.8-1.9}B_2O_{4.2-4.5}$, but these values have high uncertainties due to the small ionization cross sections of boron and oxygen. TOF-ERDA (Ref. 44) was carried out to obtain more precise compositions. Films grown at 300, 325, and 350 °C afforded compositions of $Mn_{2.4}B_2O_{6.6}$, $Mn_{2.9}B_2O_{7.5}$, and $Mn_{2.4}B_2O_{6.7}$. Among various known borates, these values are closest to $Mn_3(BO_3)_2$.[17] The compositions could also correspond to a mixed phase containing MnB_2O_4 and MnO_2. The x-ray diffraction spectra did not show any reflections for manganese borate phases, either in the as deposited film or upon annealing up to 1100 °C. However, the films also did not show any reflections for crystalline MnO_2. The films contained significant carbon ($C_{0.10-0.14}$ vs $B_{1.00}$) and hydrogen ($H_{0.62-0.78}$ vs $B_{1.00}$), but the concentrations of these elements decreased deeper in the films. Consistent with the XPS data, the carbon and hydrogen likely correspond to loosely bound surface hydrocarbon species. Additionally, the TOF-ERDA data show that the surface regions of the films have boron to manganese ratios that are closer to 1, which agree with the XPS surface compositions.

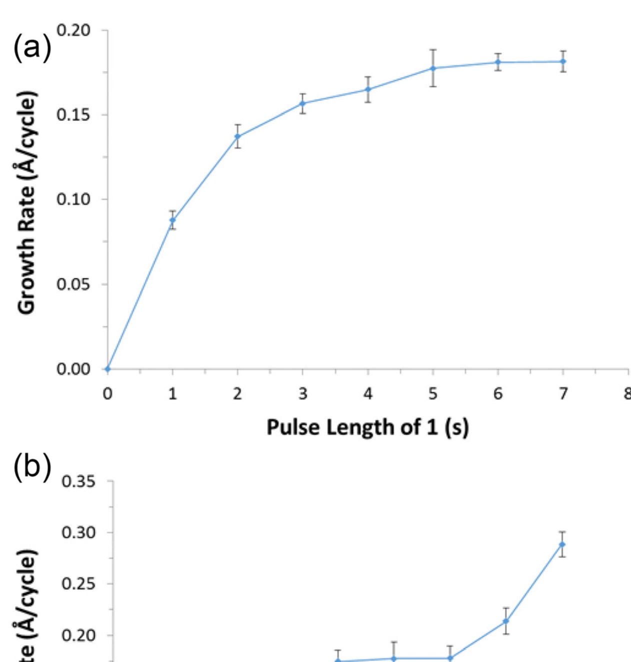

Fig. 2. (Color online) (a) Growth rate vs pulse length of 1 at 325 °C. (b) Growth rate vs deposition temperature with 1 and ozone.

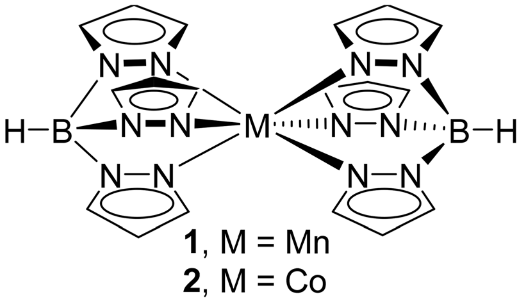

Fig. 1. Structure of **1** and **2**.

Redistribution subject to AVS license or copyright; see http://scitation.aip.org/termsconditions. IP: 130.234.75.50 On: Mon, 12 Sep 2016 08:58:03

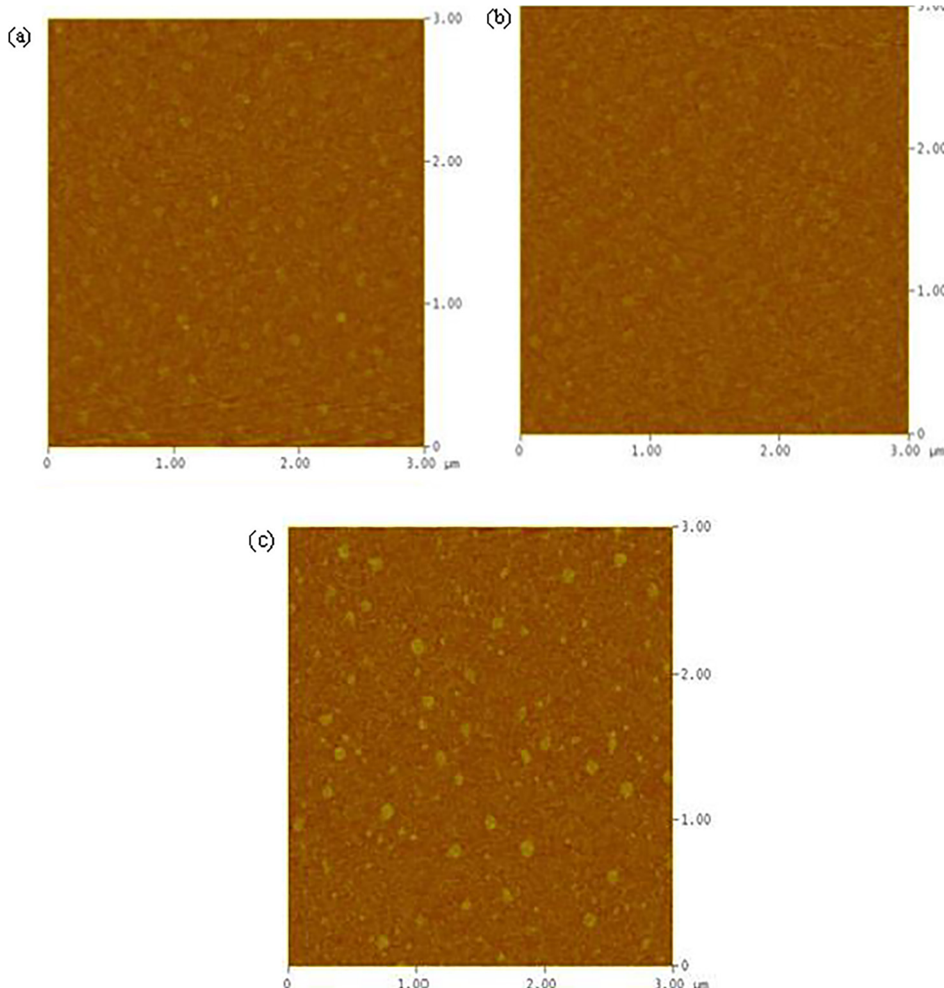

FIG. 3. (Color online) AFM images of 3 μm^2 regions of films grown from **1** and ozone on Si(100) for 2000 cycles: (a) 300 °C, (b) 325 °C, and (c) 350 °C.

C. CoB_2O_4 film growth and analysis

For comparison, cobalt borate films grown by an analogous process using **2** and ozone were explored at 325 °C. A full ALD growth study was not conducted, but saturative growth was demonstrated and a linear relationship was found between the film thickness and number of cycles. Figure 4 shows a plot of growth rate versus pulse length of **2** at 325 °C on Si(100) substrates with a native oxide layer. A growth rate of 0.39 Å/cycle was observed. Similar saturative behavior was observed with ≥2.0 s pulses of ozone at 325 °C. Based upon these experiments, a pulse sequence of **2** (6.0 s)/N_2 purge (5.0 s)/ozone (5.0 s)/N_2 purge (5.0 s) was used to construct the thickness versus number of cycles plot at 325 °C. This plot was linear and showed a growth rate of 0.42 Å/cycle, which is approximately twice that observed for the analogous process using **1** and ozone.

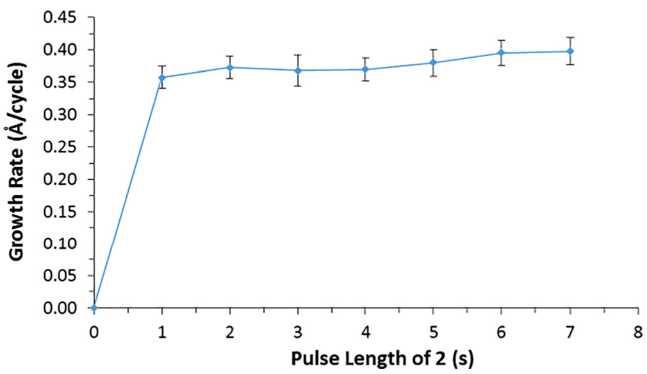

FIG. 4. (Color online) Growth rate vs pulse length of **2** at 325 °C.

Films grown at 325 °C were smooth and of uniform thickness by cross-sectional SEM. Compositional analyses were performed on 78 nm thick films deposited at 325 °C. XPS analysis showed a composition of $Co_{1.4}B_2O_{4.5}$ after 2 min of argon ion sputtering, whereas TOF-ERDA afforded a composition of $Co_{1.0}B_2O_{4.1}$. Unlike the manganese borate films, the boron to cobalt ratio was constant throughout the film. Carbon, nitrogen, and hydrogen levels were below the detection limits of XPS (carbon, nitrogen <0.5%) and TOF-ERDA (carbon, nitrogen <0.1%; hydrogen <0.3%). Based upon these analyses, films of the approximate composition CoB_2O_4 are deposited from **2** and ozone at 325 °C.

D. Discussion

The present work documents the ALD growth of films with the approximate stoichiometries $Mn_3(BO_3)_2$ and

Redistribution subject to AVS license or copyright; see http://scitation.aip.org/termsconditions. IP: 130.234.75.50 On: Mon, 12 Sep 2016 08:58:03

CoB_2O_4 from MTp_2 and ozone. These are the first examples of the vapor phase growth of first row transition metal borate films. The processes give different borate stoichiometries. With **2**, high purity CoB_2O_4 films are obtained. This stoichiometry is analogous to those obtained in the ALD growth of MB_2O_4 films (M = Ca, Sr, Ba) from $CaTp_2$, $SrTp_2$, and $Ba(TpEt_2)_2$ with water.[29–31] Replication of the 2:1 boron to cobalt ratio of **2** in the CoB_2O_4 films implies that **2** physisorbs in a molecular fashion to the surface of the growing film, and is then efficiently transformed by ozone to CoB_2O_4. In contrast, **1** and ozone afford films of the approximate composition $Mn_3(BO_3)_2$, with an approximate 3:2 manganese to boron stoichiometry. The data suggest that **1** chemisorbs to the surface of the growing film with approximate loss of one Tp ligand per molecule of **1**. Subsequent treatment with ozone then leads to manganese borate films. As a comparison, ALD growth using $Mn(thd)_3$ and ozone afforded MnO_2 films within an ALD window of 140–230 °C.[45,46] In the present manganese borate ALD process, the ozone pulses may oxidize surface-bound MnTp species to manganese(IV) borates that also contain oxo ligands. Since high valent manganese oxides are strong oxidants,[45,46] the subsequent pulse of **1** likely leads to oxidation of one Tp ligand by the surface oxo groups and loss of volatile products that remove an average of one boron atom per molecule of **1**. In contrast to the range of higher oxidation state manganese oxides, cobalt oxides are limited to CoO and Co_3O_4,[47] neither of which is a strong oxidant. Accordingly, **2** physisorbs molecularly to the surface of the growing film and is transformed to CoB_2O_4 upon subsequent treatment with ozone. The large difference in growth rate between the manganese borate (0.18–0.19 Å/cycle) and cobalt borate (0.39–0.42 Å/cycle) processes may arise because multiple higher valent manganese-oxygen bonds are required to oxidize the Tp ligand in **1**, thereby reducing the surface coverage of MnTp fragments. In contrast, **2** appears to physisorb molecularly, providing a higher surface coverage in the monolayer.

The processes described herein demonstrate rare control of thin film stoichiometries in ALD that are governed by the elements present in a single precursor. In particular, deposition of manganese borate films from **1** demonstrates that intermediate oxidizing surfaces obtained with ozone can lead to borate film stoichiometries that differ from the boron to manganese ratio that is present in precursor **1**. Bimetallic precursors have been previously used in ALD in attempts to control the concentrations of two elements in the thin films, but generally afford poor stoichiometric control. Single precursors containing 1:2 strontium to tantalum ratios were employed for the ALD growth of Sr-Ta-O films,[35,36] but strontium to tantalum ratios ranging from 0.5 to 1.5 were obtained in films under various deposition conditions. The lack of stoichiometric control could arise from the formation of volatile tantalum oxides.[36] $PrAlO_x$ and $NdAlO_x$ films were grown by ALD with 1:1 neodymium/praseodymium to aluminum bimetallic isopropoxide precursors, but nonstoichiometric praseodymium to aluminum and neodymium to aluminum ratios (0.30–0.71) resulted.[37] $Bi(CH_2SiMe_3)_3$ and ozone were used for the ALD growth of Bi-Si-O films,[38] but the silicon to bismuth ratio increased from 1.5 to 5.0 between 200 and 450 °C.

IV. SUMMARY AND CONCLUSIONS

The ALD growth of manganese and cobalt borate films was demonstrated using **1** or **2** with ozone on Si(100) substrates with native oxide. Self-limited growth was established at 325 °C with 5.0 and 6.0 s pulse lengths of **1** and **2**, respectively, and 5.0 s pulse lengths of ozone. The manganese borate process afforded an ALD window between 300 and 350 °C. Plots of thickness versus number of cycles were linear for both processes. Film compositions were determined using a combination of XPS and TOF-ERDA measurements. With the cobalt borate process, the 2:1 boron to cobalt ratio present in precursor **2** was replicated in the thin film, suggesting that **2** physisorbs to the surface of the growing film and is then transformed to CoB_2O_4 upon treatment with ozone. In contrast, the 2:1 boron to manganese ratio present in **1** is transformed to the approximate 3:2 boron to manganese ratio in $Mn_3(BO_3)_2$ or mixed MnB_2O_4/MnO_2 films upon treatment with ozone. The differing stoichiometries in films derived from **1** or **2** and ozone are proposed to arise from the oxidizing ability of the intermediate high valent manganese oxide layers, which afford oxidation of one Tp ligand by the surface oxo groups and loss of volatile products that remove an average of one boron atom per molecule of **1**. In contrast, intermediate cobalt oxide layers have low oxidizing power, which leads to physisorption of **2** and conversion to CoB_2O_4 upon treatment with ozone. The present study describes the gas phase deposition of transition metal borate films with well-defined stoichiometries, which should allow these materials to be explored in catalysis, lithium ion batteries, and other applications.

ACKNOWLEDGMENTS

The authors gratefully acknowledge generous support from the U.S. Army Research Office (Grant No. W911NF-12-10313), the U.S. National Science Foundation (Grant No. CHE-1212574), and SAFC Hitech.

[1] D. N. Nikogosyan, *Nonlinear Optical Crystals: A Complete Survey* (Springer, New York, 2005).
[2] C. Chen, Z. Lin, and Z. Wang, Appl. Phys. B **80**, 1 (2005).
[3] D. A. Keszler, Curr. Opin. Sol. State Mater. Sci. **1**, 204 (1996).
[4] P. Becker, Adv. Mater. **10**, 979 (1998).
[5] A. M. Smith, L. Trotochaud, M. S. Burke, and S. W. Boettcher, Chem. Commun. **51**, 5261 (2015).
[6] C. L. Farrow, D. K. Bediako, Y. Surendranath, D. G. Nocera, and S. J. L. Billinge, J. Am. Chem. Soc. **135**, 6403 (2013).
[7] S. K. Choi, W. Choi, and H. Park, Phys. Chem. Chem. Phys. **15**, 6499 (2013).
[8] T. Jin, P. Diao, D. Xu, and Q. Wu, Electrochim. Acta **114**, 271 (2013).
[9] D. K. Bediako, Y. Surendranath, and D. G. Nocera, J. Am. Chem. Soc. **135**, 3662 (2013).
[10] M. T. Winkler, C. R. Cox, D. G. Nocera, and T. Buonassisi, PNAS **110**, E1076 (2013).
[11] D. K. Bediako, B. Lassalle-Kaiser, Y. Surendranath, J. Yano, V. K. Yachandra, and D. G. Nocera, J. Am. Chem. Soc. **134**, 6801 (2012).
[12] Y. Surendranath, D. K. Bediako, and D. G. Nocera, PNAS **109**, 15617 (2012).

Redistribution subject to AVS license or copyright; see http://scitation.aip.org/termsconditions. IP: 130.234.75.50 On: Mon, 12 Sep 2016 08:58:03

[13]A. J. Esswein, Y. Surendranath, S. Y. Reece, and D. G. Nocera, Energy Environ. Sci. **4**, 499 (2011).
[14]S. Y. Reece, J. A. Hamel, K. Sung, T. D. Jarvi, A. J. Esswein, J. J. H. Pijpers, and D. G. Nocera, Science **334**, 645 (2011).
[15]M. Dinča, Y. Surendranath, and D. G. Nocera, PNAS **107**, 10337 (2010).
[16]Y. Surendranath, M. Dinča, and D. G. Nocera, J. Am. Chem. Soc. **131**, 2615 (2009).
[17]B. Le Roux, C. Bourbon, O. I. Lebedev, J.-F. Colin, and V. Pralong, Inorg. Chem. **54**, 5273 (2015).
[18]P. Barpanda, D. Dwibedi, S. Ghosh, Y. Kee, and S. Okada, Ionics **21**, 1801 (2015).
[19]J. Mun, J. Lee, T. Hwang, J. Lee, H. Noh, and W. Choi, J. Electroanal. Chem. **745**, 8 (2015).
[20]S. Afyon, D. Kundu, A. J. Darbandi, H. Hahn, F. Krumeich, and R. Nesper, J. Mater. Chem. A **2**, 18946 (2014).
[21]S. Afyon, M. Wörle, and R. Nesper, Angew. Chem. Int. Ed. **52**, 12541 (2013).
[22]K.-J. Lee, L.-S. Kang, S. Uhm, J. S. Yoon, D.-W. Kim, and H. S. Hong, Curr. Appl. Phys. **13**, 1440 (2013).
[23]A. M. Ozera, V. I. Simagina, O. V. Komova, O. V. Netskina, G. V. Odegova, O. A. Bulavchenko, and N. A. Rudina, J. Alloys Compd. **513**, 266 (2012).
[24]Y. Wang, J. Feng, B. Feng, X. Song, and J. Cao, RSC Adv. **5**, 28950 (2015).
[25]D. B. Studebaker, G. T. Stauf, T. H. Baum, T. J. Marks, H. Zhou, and G. K. Wong, Appl. Phys. Lett. **70**, 565 (1997).
[26]G. Malandrino, R. Lo Nigro, and I. L. Fragalà, Inorg. Chim. Acta **360**, 1138 (2007).
[27]G. Malandrino, R. Lo Nigro, and I. L. Fragalà, Chem. Vap. Deposition **13**, 651 (2007).
[28]M. J. Saly, M. J. Heeg, and C. H. Winter, Inorg. Chem. **48**, 5303 (2009).
[29]M. J. Saly, F. Munnik, and C. H. Winter, J. Mater. Chem. **20**, 9995 (2010).
[30]M. J. Saly, F. Munnik, and C. H. Winter, Chem. Vap. Deposition **17**, 128 (2011).
[31]M. J. Saly, F. Munnik, R. J. Baird, and C. H. Winter, Chem. Mater. **21**, 3742 (2009).
[32]S. M. George, Chem. Rev. **110**, 111 (2010).
[33]M. Leskelä and M. Ritala, Angew. Chem. Int. Ed. **42**, 5548 (2003).
[34]K. Gregorczyk and M. Knez, Prog. Mater. Sci. **75**, 1 (2016).
[35]M. Likosius, C. Wenger, S. Pasko, I. Costina, J. Dabrowski, R. Sorge, H.-J. Müssig, and C. Lohe, IEEE Trans. Electron Devices **55**, 2273 (2008).
[36]M. Vehkamäki, M. Ritala, M. Leskelä, A. C. Jones, H. O. Davies, T. Sajavaara, and E. Rauhala, J. Electrochem. Soc. **151**, F69 (2004).
[37]J. M. Gaskell, S. Przybylak, A. C. Jones, H. Aspinall, P. R. Chalker, K. Black, R. J. Potter, P. Taechakumput, and S. Taylor, Chem. Mater. **19**, 4796 (2007).
[38]J. Harjuoja, T. Hatanpää, M. Vehkamäki, S. Väyrynen, M. Putkonen, L. Niinistö, M. Ritala, M. Leskelä, and E. Rauhala, Chem. Vap. Deposition **11**, 362 (2005).
[39]See supplementary material at http://dx.doi.org/10.1116/1.4961385 for the precursor properties of **1** and **2**, ALD growth data, and film characterization.
[40]S. Trofimenko, J. Am. Chem. Soc. **89**, 3170 (1967).
[41]C. D. Wagner, W. M. Riggs, L. E. Davis, J. F. Moulder, and G. E. Murlenberg, *Handbook of X-ray Photoelectron Spectroscopy* (Perkin-Elmer Corporation, Eden Prairie, MN, 1979).
[42]T. Kitano, Y. Sohrin, Y. Hatay, H. Kawasaki, T. Hori, and K. Ueda, J. Chem. Soc., Dalton Trans. 3564 (2001).
[43]M. R. Churchill, K. Gold, and C. E. Maw, Jr., Inorg. Chem. **9**, 1597 (1970).
[44]M. Laitinen, M. Rossi, J. Julin, and T. Sajavaara, Nucl. Instrum. Methods, B **337**, 55 (2014).
[45]O. Nilsen, H. Fjellvåg, and A. Kjekshus, Thin Solid Films **444**, 44 (2003).
[46]O. Nilsen, S. Foss, H. Fjellvåg, and A. Kjekshus, Thin Solid Films **468**, 65 (2004).
[47]N. N. Greenwood and A. Earnshaw, *Chemistry of the Elements*, 2nd ed. (Elsevier, Amsterdam, 1997), pp 1119–1120.

Redistribution subject to AVS license or copyright; see http://scitation.aip.org/termsconditions. IP: 130.234.75.50 On: Mon, 12 Sep 2016 08:58:03